

# Imaging of skull base: Pictorial essay

Abhijit A Raut, Prashant S Naphade<sup>1</sup>, Ashish Chawla<sup>2</sup>

Department of Radiology, Seven Hills Hospital, Mumbai, <sup>1</sup>Department of Radiology, Employee's State Insurance Corporation Hospital, Mumbai, Maharashtra, <sup>2</sup>Department of Radiology, Sri Aurobindo Medical College and Postgraduate Institute, Indore, Madhya Pradesh, India

**Correspondence:** Dr. Abhijit Raut, Department of Radiology, Seven Hills Hospital, Marol Maroshi Road, Andheri East, Mumbai - 400 059, India. E-mail: abhijitaraut@gmail.com

## Abstract

The skull base anatomy is complex. Numerous vital neurovascular structures pass through multiple channels and foramina located in the base skull. With the advent of computerized tomography (CT) and magnetic resonance imaging (MRI), accurate preoperative lesion localization and evaluation of its relationship with adjacent neurovascular structures is possible. It is imperative that the radiologist and skull base surgeons are familiar with this complex anatomy for localizing the skull base lesion, reaching appropriate differential diagnosis, and deciding the optimal surgical approach. CT and MRI are complementary to each other and are often used together for the demonstration of the full disease extent. This article focuses on the radiological anatomy of the skull base and discusses few of the common pathologies affecting the skull base.

**Key words:** Computed tomography; magnetic resonance imaging; skull base

## Introduction

The skull base forms the floor of the cranial cavity that separates brain from facial structures and suprahyoid neck. The skull base anatomy is complex and is not directly accessible for clinical evaluation. Surgical exploration without accurate knowledge of anatomy can be catastrophic. The recent advances in neuroimaging has contributed significantly to the development of modern-day surgical approach and targeted radiotherapy of the skull base pathologies, which result in improvement of anatomic access for resection and reconstruction with minimal functional and aesthetic morbidity and mortality.

Imaging plays vital role in diagnosis of certain pathologies, preoperative staging of neoplasms, defining tumor extension and spread, planning surgical approach, detection of tumor recurrences, and follow up.

The skull base is composed of five bones: (1) ethmoid, (2) sphenoid, (3) occipital, (4) paired temporal, and (5) paired frontal bones. Three naturally contoured regions can be identified when skull base is viewed from above [Figure 1]. These are the anterior, middle, and posterior cranial fossae. However, there are no separate boundaries corresponding to these fossae when seen from below [Figure 2]. Numerous foramina and canals are seen in the skull base, which transmit vital neurovascular structures [Figures 3-9].

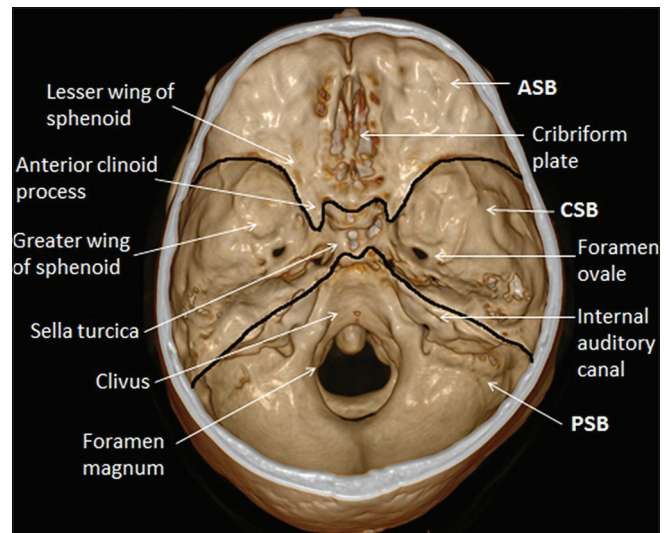


**Figure 1:** Endocranial aspect of skull base showing subdivisions of skull base

Access this article online	
Quick Response Code:	Website: www.ijri.org
	DOI: 10.4103/0971-3026.111485

CT and MRI are the imaging modality of choice for evaluation of skull base anatomy and pathology. This brief review article discusses common skull base pathologies along with the relevant anatomy and imaging techniques.

## Relevant Anatomy

### Anterior skull base (ASB)

The ASB forms the bottom of the anterior skull, separating the anterior cranial fossa from the paranasal sinuses and the orbits. The anterior border of ASB is formed by the posterior wall of the frontal sinus and posterior border is formed by the lesser wing of the sphenoid bone and anterior clinoid processes. The floor of the ASB is formed by roof of the nasal cavity and ethmoid sinuses medially. The cribriform plate of the ethmoid bone has multiple small perforations that transmit olfactory nerves from the nasal mucosa to the olfactory bulb. The lateral wall of the ASB is formed by thick and strong orbital plates of the frontal bone, which contributes to the largest surface area of the anterior cranial fossa.<sup>[1]</sup>

The site where the anterior ethmoid artery enters the anterior cranial fossa (lateral lamella of the cribriform plate) is the site of common bony injuries and cerebrospinal fluid (CSF) leaks.<sup>[1]</sup>

### Central skull base (CSB)

The CSB makes up the floor of the middle cranial fossa. The

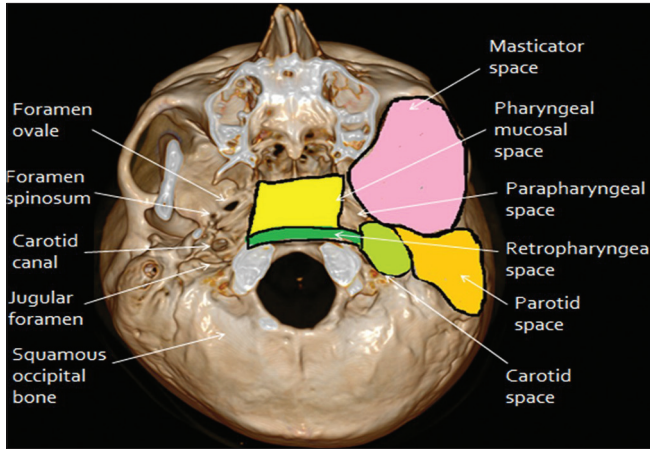


**Figure 2:** Exocranial aspect of skull base showing attachment of deep neck spaces to skull base

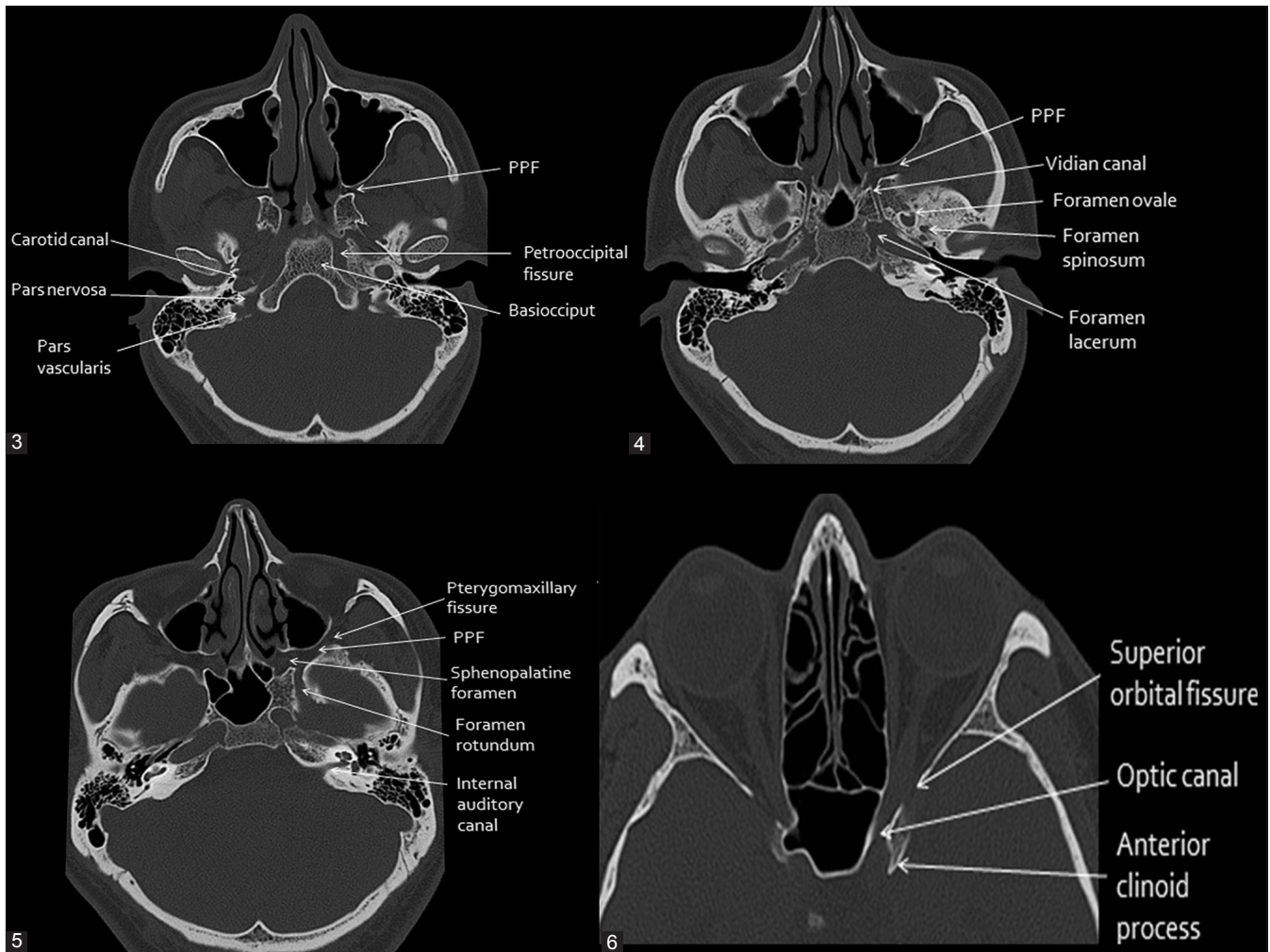


**Figure 3-6:** Axial CT bone window of skull base from inferior to superior aspect showing major apertures of skull base

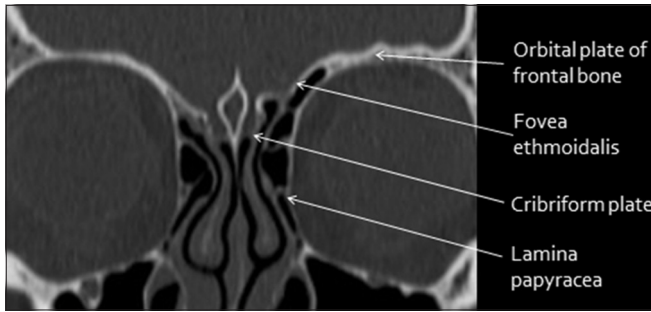


Figure 7: Coronal CT bone window of anterior skull base

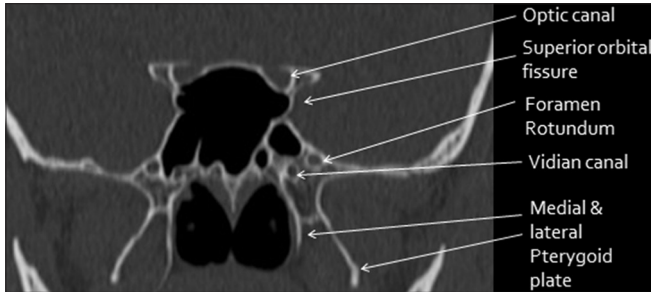


Figure 8: Coronal CT bone window of central skull base

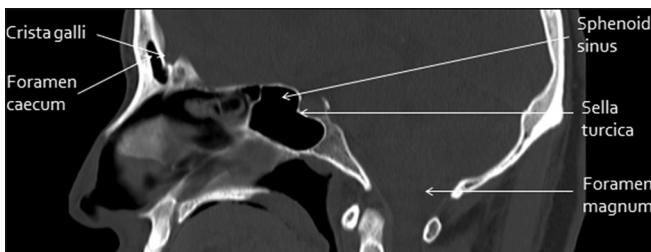


Figure 9: Sagittal CT bone window of skull base

sphenoid bone contributes to the most of the CSB. Anterior border of the CSB is formed by the tuberculum sellae, anterior clinoid processes, posterior margin of the lesser sphenoid wings, and the anterior and superior rim of the greater sphenoid wings. Posterior border of CSB is formed by superior borders of the petrous part of the temporal bone and the dorsum sellae of the sphenoid.<sup>[2]</sup>

The central part of middle cranial fossa is formed by the body of sphenoid. The sella turcica is a depression in the superior surface of the body of sphenoid bone for pituitary gland. It is bordered anteriorly by tuberculum sellae and posteriorly by dorsum sellae. Floor of the sella is formed by the sphenoid sinus. The roof of the sella turcica is formed by a fold of dura called diaphragma sellae, which is pierced by the pituitary stalk. The CSB is further divided into midline sagittal, off-midline parasagittal, and lateral compartments by drawing two vertical lines passing medially to the petroclival fissure and just lateral to the foramen ovale, respectively.<sup>[3]</sup>

The midline sagittal compartment includes the body of the sphenoid and the portion of the clivus anterior to the

spheno-occipital synchondrosis (basisphenoid).<sup>[3]</sup>

Important components of the parasagittal compartment include the petroclival synchondrosis, foramen lacerum, and medial aspect of the greater sphenoid wing. Many crucial neurovascular structures lay in this compartment, which includes cavernous sinus, superior orbital fissure, foramen rotundum, vidian canal, and foramen lacerum. The cavernous sinus forms the superior and medial boundary of the parasagittal compartment while the parapharyngeal and masticator spaces of the suprahyoid neck are along the inferior aspect.<sup>[3]</sup>

Lateral compartment of the central skull base is formed by sphenoid triangle, squamous part of temporal bone, and temporomandibular joint.<sup>[3]</sup>

## Important Anatomical Landmarks in Central Skull Base

### Cavernous sinus (CS)

The CS is composed of a network of small venous channels that may arbitrarily be divided into different compartments. The CS extends from the orbital apex and superior orbital fissure anteriorly to the Meckel's cave. The CS connects the superior and inferior ophthalmic veins, pterygoid plexus, and Sylvian vein to superior and inferior petrosal sinuses.

The internal carotid artery (ICA) is the medial most structure inside the CS. Cranial nerves III and IV and the first and second divisions of the cranial nerve V (from superior to inferior) are located in the lateral dural wall of the CS. Cranial nerve VI courses in the central part of the CS inferolateral to the ICA.

### Optic canal

The optic canal is formed by the lesser wing of sphenoid and transmits cranial nerve II and the ophthalmic artery.

### Superior orbital fissure

The superior orbital fissure is located between the greater and lesser wings of the sphenoid bone. The sphenoid body is located medial to the SOF. SOF transmits cranial nerves III, IV, VI, and V1.

Optic strut separates the optic canal from the superior orbital fissure. The optic canal and the superior orbital fissure together form the orbital apex, one of the important transition zones between intracranial and extracranial contents.

### Foramen rotundum

The foramen rotundum is seen inferior to the superior orbital fissure and it transmits cranial nerve V2. It connects the cavernous sinus in the middle cranial fossa to the pterygopalatine fossa.

**Vidian canal**

The vidian canal is located in the floor of the sphenoid sinus at the junction of the pterygoid process and the sphenoid body connecting the pterygopalatine fossa anteriorly and the foramen lacerum posteriorly. The vidian canal transmits the vidian artery (branch of the maxillary artery), and also transmits the vidian nerve (formed by the greater superficial petrosal nerve and the deep petrosal nerve).

**Foramen spinosum**

It is an aperture in the greater wing of the sphenoid posterolateral to foramen ovale that gives passage to the middle meningeal artery.

**Pterygopalatine fossa (PPF)**

The PPF is a pyramidal space located inferior to the orbital apex and posterior to the maxillary sinus. It contains maxillary nerve, the pterygopalatine ganglion, and terminal branches of the internal maxillary artery. It is bound posteriorly by the pterygoid plates, medially by the palatine bone, and anteriorly by the maxillary sinus.<sup>[4]</sup>

Laterally, it communicates with the infratemporal fossa via the pterygomaxillary fissure. It also connects with the nasal cavity medially via the sphenopalatine foramen, the orbit via the inferior orbital fissure, and intracranial space via the foramen rotundum. Posteriorly, the anterior opening of the vidian canal permits the entrance of the vidian nerve, which constitutes the preganglionic parasympathetic component of the pterygopalatine ganglion. Inferiorly, the descending pterygoid canal leads to the greater and lesser palatine foramina, which access the palate.

On CT and MRI, PPF is identified as a fat-filled space between the pterygoid plates and the posterior wall of maxillary sinus. Replacement of normal fat signal intensity on T1-weighted MR images and abnormal enhancement or widening of the PPF indicates local extension. Infiltration of PPF by tumor indicates bad prognosis.<sup>[2]</sup>

**Posterior skull base (PSB)**

The anterior margin of the PSB is formed by the posterior surface of the clivus. The clivus is formed from fusion of the basisphenoid and basiocciput. The lateral portion of posterior skull base is formed by the posterior surface of the petrous temporal bone superiorly and the condylar part of the occipital bone inferiorly. The mastoid temporal bone and the squamous occipital bone form the posterior portion of the PSB.<sup>[5]</sup>

The foramen magnum is entirely formed within the occipital bone. Important structures transmitting through the foramen magnum are medulla oblongata, vertebral arteries, anterior/posterior spinal arteries, and spinal accessory nerve.

The jugular foramen is seen at the posterior end of

petro-occipital suture. Anteriorly the caroticojugular spine separates the jugular foramen from the inferior carotid opening. Along the medial aspect, an osseous bony bar called the jugular tubercle separates the jugular foramen from the hypoglossal canal, which transmits hypoglossal nerve.

Fibrous or bony septum divides jugular foramen into anteromedial pars nervosa and posterolateral pars vascularis. Pars nervosa is smaller and more consistent in size, and transmits cranial nerve IX (glossopharyngeal nerve) with its tympanic branch (Jacobson nerve) and the inferior petrosal sinus. The pars vascularis is larger and more variable in size, transmitting the internal jugular vein, cranial nerve X (vagus nerve) with its auricular branch (Arnold nerve), cranial nerve XI (accessory nerve), and the posterior meningeal artery. The appearance of the jugular foramen is anatomically variable, and sometimes both cranial nerves IX and X traverse through the pars nervosa. The right jugular foramen is larger than the left in 75% of the population. When the roof of the jugular bulb is seen above the level of floor of internal auditory canal, it is called a high-riding jugular bulb, which is more common on the right side. This is a dangerous variant and compromises the exposure during translabyrinthine surgery.<sup>[1]</sup>

**Relation of skull base to the deep facial spaces**

The deep facial spaces are in close contact with the base skull. Infections and tumors of these spaces often extend up to the skull base. Hence it is important for the radiologist to know the relation of the skull base to the deep facial planes. Parapharyngeal, masticator, carotid, and retropharyngeal spaces are seen in close contact with the skull base along their cephalad aspect.

Parapharyngeal space extends caudally to the submandibular space and cranially abuts the base skull. It contains fat within, which acts as a medium for infection. Tumors can easily traverse across the fat within the parapharyngeal space.

Masticator space connects the mandible to the skull base. Odontogenic infections and oropharyngeal squamous cell carcinoma can tract along masticator space to the base skull. Intracranial extension of the tumor can occur via third division of trigeminal nerve, mandibular nerve (perineural spread) through the foramen ovale.

Vascular lesions such as jugular vein thrombosis and neural tumors such as schwannoma, neurofibroma, and paraganglioma are seen in the carotid space. These lesions usually spread longitudinally along the length of the neck with subsequent extension into the jugular foramina in the skull base.

## Imaging Modalities and Techniques

Different protocols are being used for evaluation of skull base. CT and MR imaging are complementary to each other and are often used together for the diagnosis of skull base diseases. With the advent of multislice CT scanners, it is possible to acquire 0.5- to 0.6-mm-thin section of base skull and perform multiplanar reconstruction. The images are reviewed using bone window and soft tissue algorithm. Postcontrast evaluation may be performed especially when vascular mass is suspected.<sup>[6]</sup>

CT is the modality of choice in defining the bony anatomy of the skull base and to depict the thin cortical margins of skull base neurovascular foramina. CT is more sensitive in detecting fibro osseous skull base lesions, calcification, and sclerosis. CT scan is the gold standard technique for evaluation of base skull fractures and to detect CSF leak.

MRI has an edge over CT scan to depict intracranial extent (dural, leptomeningeal and brain parenchyma invasion), perineural and perivascular spread, and bone marrow involvement. Axial and coronal images using fast spin echo T1 and T2 W images should be obtained with fat-suppressed, postcontrast images using a smaller field of view with a slice thickness of 3 mm. Additional short-tau inversion recovery (STIR) images are obtained. STIR images have better fat suppression but take longer time and are susceptible to pulsatile flow artifacts. Gradient echo T2\* images may be useful to demonstrate paramagnetic substances, such as calcifications, blood degradation products, or melanin within a lesion.<sup>[6]</sup> Diffusion weighted images are helpful in differentiating malignant tumors from benign based on ADC values.<sup>[7]</sup>

### General imaging considerations

A large number of tumors can involve in the base skull. The role of imaging is to detect the location and extension of mass, differentiate benign from malignant tumors, to look for resectability, meningeal or brain parenchymal invasion, invasion of orbit, cavernous sinus or vascular structures, and perineural spread.

MRI with postcontrast evaluation is usually performed for evaluation of skull base lesions. Plain CT scan provides additional bony details. CT and MRI are complimentary to each other and together can provide the vital information to the surgeon to decide the possibility of resectability and best surgical approach.<sup>[2]</sup>

CT scan provides information about bony anatomy, pattern of bone destruction, periosteal reaction [Figure 10], sclerosis, ossification, and calcification. Aggressive infections and malignant lesions show permeative and erosive patterns of bone involvement while smooth cortical expansion and remodeling with cortical thinning is associated with benign slow growing processes. Phlebolith formation is associated



**Figure 10 (A, B):** Coronal (A) and sagittal (B) multiplanar reconstruction CT bone window reveal irregular perpendicular periosteal reaction (white arrow) involving orbital plate of right frontal bone with a large soft tissue mass in a proven case of round cell tumor

with vascular tumors while bone sclerosis is associated with meningiomas.<sup>[1]</sup>

MRI has an edge over CT in tissue characterization. In general, inflammatory lesions have high water content and have high T2W signal intensity. Benign and low-grade tumors of minor salivary glands, schwannoma, hemangioma, and meningioma have high T2W signal. Malignant neoplasms are cellular and have intermediate signal intensity on T2W images. Apparent diffusion coefficient (ADC) values within malignant lesions are decreased compared with nonmalignant tissue. At 1.5 T, an ADC value of  $1.22 \times 10^{-3} \text{ mm}^2/\text{s}$  and that on 3T scanners  $1.3 \times 10^{-3} \text{ mm}^2/\text{s}$  is suggested as a possible threshold for distinguishing benign from malignant lesions.<sup>[7]</sup>

### PET CT

The high degree of metabolic activity within most malignant tumors is detected on PET CT and metastatic deposits far from the primary site. Also recurrence and postsurgical fibrosis can be differentiated from the primary tumor easily. However, intense physiological uptake by the brain is the limitation in evaluation of base skull lesions.

### Location and extension of the lesion

Exact location and extent of the lesion is essential to determine the best surgical approach for excision or biopsy. Contraindications for surgical excision may vary. Lateral or superior wall of sphenoid sinus invasion, infiltration into cavernous sinus, bilateral optic nerves or optic chiasma involvement, nasopharynx and prevertebral fascia are common contraindications for complete surgical excision.<sup>[2]</sup>

### Dural invasion

When dural invasion is present, a combined craniofacial approach is recommended. The 5-year survival rate is significantly decreased in the presence of dural invasion. Nodular dural enhancement and linear dural enhancement thicker than 5 mm when seen indicate dural invasion [Figure 11]. Dural enhancement less than 5 mm may be seen in reactionary fibrovascular changes and may not suggest dural invasion.<sup>[6]</sup>

### Orbital invasion

Sinus lesions may easily infiltrate the orbit wall through the lamina papyracea, which is the weakest of all orbital walls [Figure 12]. However, the CSB lesions invade the orbit through the orbital fissures or orbital apex. Loss of fat and abnormal enhancement within these neural foramina indicate invasion, which can be better appreciated on MRI. Strong fibrous periorbita is attached along the superior and inferior aspect of the medial wall and limits the tumor spread. Tumors invading the periorbita and extending into the orbital apex require orbital exenteration with sacrifice of the optic nerve. Both CT and MRI are equivocal for invasion of periorbita. Tumor spreading to the orbital apex can enter into the middle cranial fossa through the superior orbital fissure.<sup>[1]</sup>

### Cavernous sinus invasion

Invasion of the cavernous sinus usually is contraindicated for complete resection of a lesion. Imaging signs of cavernous sinus invasion include compression, encasement, stenosis, or irregularity of the cavernous carotid artery; loss of contrast enhancement of the cavernous sinus, which is best depicted on a dynamic coronal MR imaging study; and

bulging of the lateral sinus wall, which is concave under normal conditions [Figure 12].<sup>[3]</sup>

### Perineural spread

Perineural spread is common in head and neck malignancies; especially seen in adenoid cystic carcinoma [Figure 11]. It can also be seen in squamous cell carcinoma, malignant melanoma, lymphoma, basal cell carcinoma, adenocarcinoma, mucoepidermoid tumor, rhabdomyosarcoma, chondrosarcoma, malignant mixed tumor, and esthesioneuroblastoma. Perineural spread is usually associated with cavernous sinus, cranial nerve infiltration, skull base invasion, and has bad prognosis.<sup>[8]</sup>

Perineural spread occurs commonly along cranial nerves V, III, IV, and VI through foramen rotundum, foramen ovale, superior and inferior orbital fissures. Perineural spread in parotid malignancies occurs along the facial nerve via stylomastoid foramen. Perineural spread along the cranial nerves IX, X, XI, and XII with intracranial extension occurs along the jugular foramen and hypoglossal canal.<sup>[8]</sup>

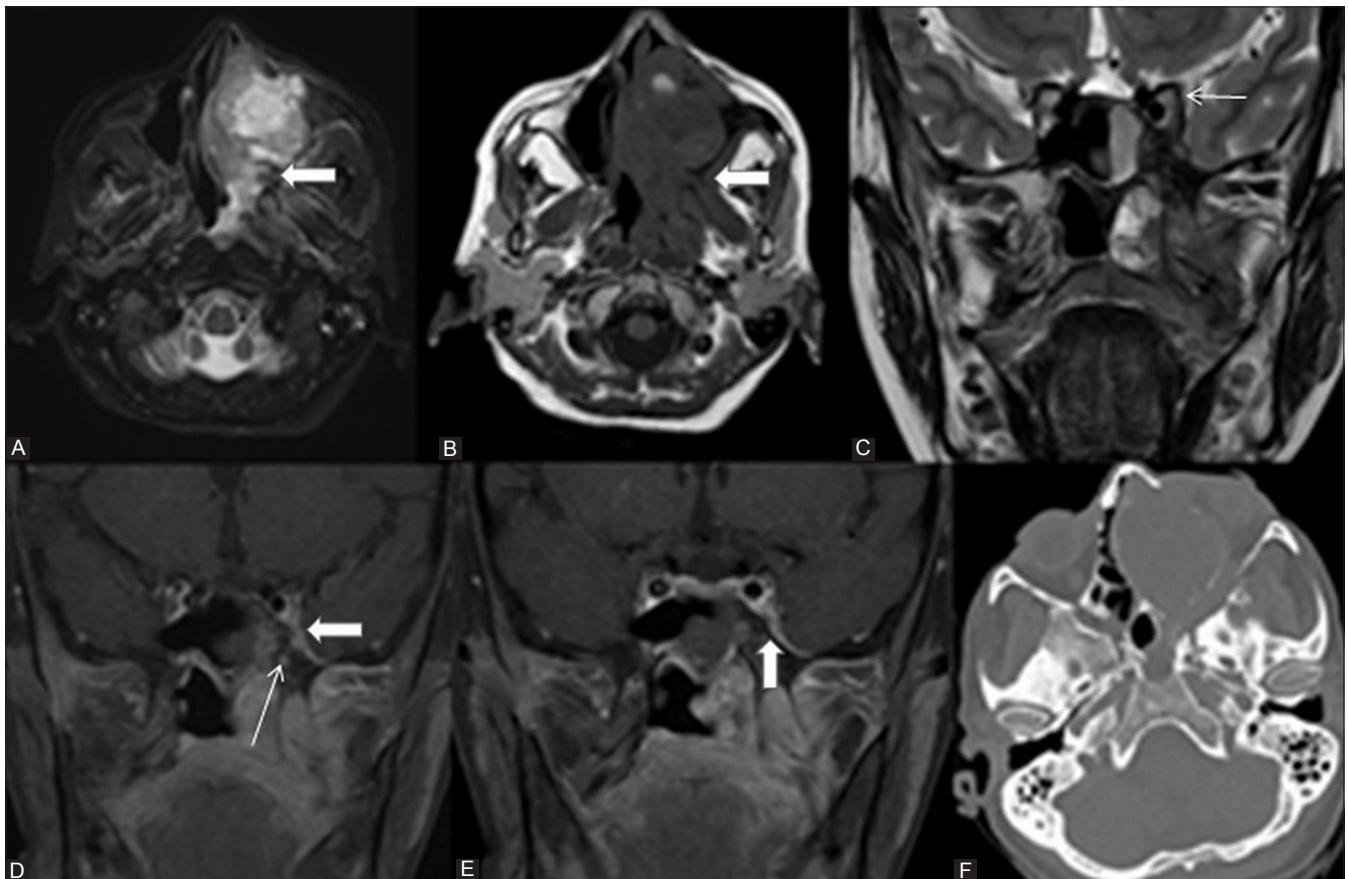


**Figure 11 (A-F):** Axial T2 (A) and T1WI (B) reveal heterogeneous mass lesion in left maxillary sinus, left nasal cavity, PPF, and masticator space in a proven case of adenoid cystic carcinoma of left maxillary sinus. Coronal T2WI (C) reveals extension of T2 hypointense mass in the left cavernous sinus. Postcontrast coronal image (D) reveals homogeneous enhancement of mass with perineural spread along maxillary nerve in foramen rotundum (thick arrow) and vidian nerve in vidian canal (thin arrow). Dural invasion is seen in postcontrast coronal image (E). Axial CT bone window (F) reveals bone destruction

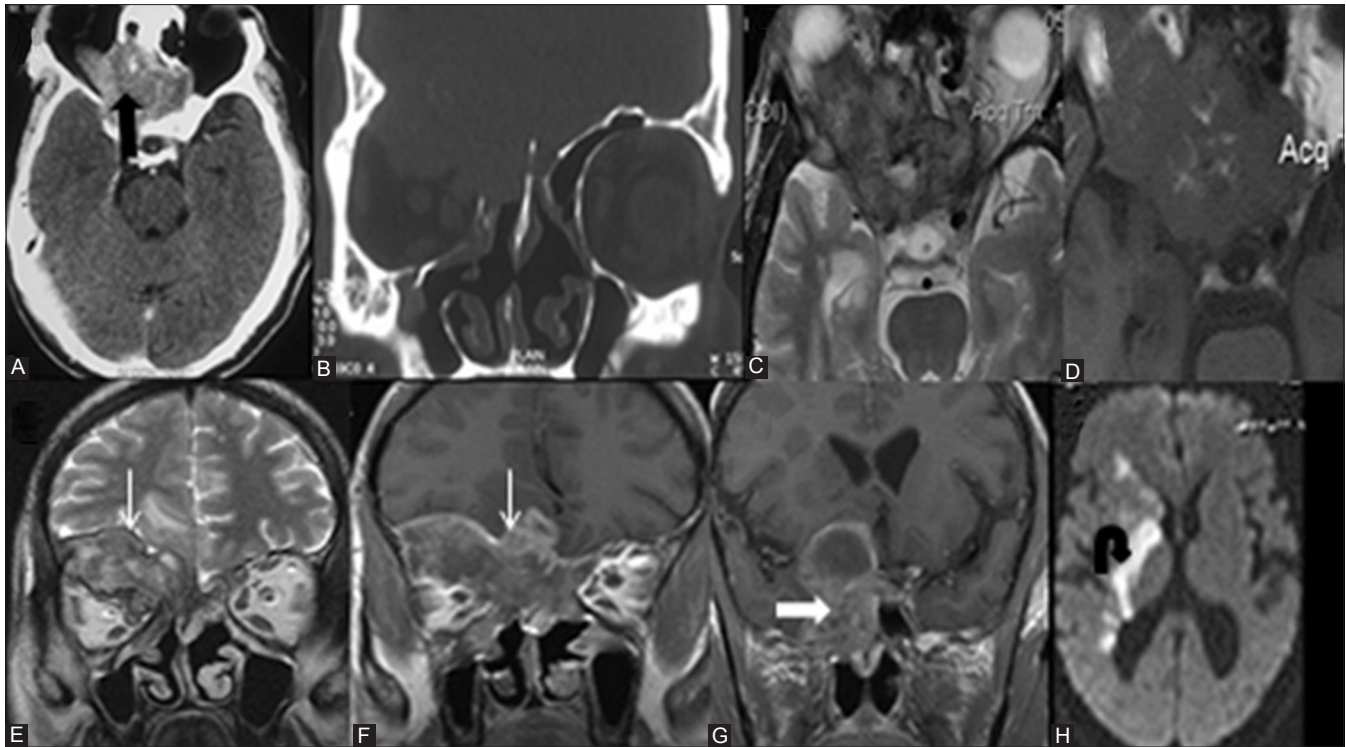


**Figure 12 (A-H):** Axial CT scan (A and B) reveal heterogeneously enhancing soft tissue in posterior ethmoid sinuses with extension into both orbits (black arrow). The soft tissue appears marked T2 hypointense (C) and T1 isointense with few hyperintense foci (D). Orbital and extradural anterior cranial fossa spread (thin white arrow) is seen on coronal T2 (E) and postcontrast T1 (F) images. Extension in right cavernous sinus (thick white arrow) is seen (G) with resultant right ICA territory infarcts (curved arrow in H)

## Classification of Skull Base Diseases

**Congenital:** Nasal glioma, Nasal dermoid, Encephalocele/ meningocele, Rathke's cleft cyst.

**Inflammation:** Infective: Pyogenic, fungal, and tuberculosis

**Noninfective:** Sarcoidosis, Wegener's granulomatosis, mucocele

**Trauma:** Fracture, CSF leaks

### Tumors seen anywhere in the base skull

**Fibro-osseous lesions:** Fibrous dysplasia, Ossifying fibroma, Osteoma, Osteoblastoma, Aneurysmal bone cyst, Paget's disease, Ewing's Sarcoma, Osteosarcoma, chondrosarcoma.

**Epithelial:** Squamous and adenocarcinoma, melanoma

**Nonepithelial:** Rhabdomyosarcoma, large cell lymphoma, meningioma, neurofibroma, schwannoma, and their malignant counterparts.

**Minor Salivary gland:** Adenoid cystic carcinoma

**Vascular malformations**

**Plasmacytoma and multiple myeloma**

**Metastasis:** Carcinoma prostate [Figure 13], breast, lung, lymphoma, melanoma, leukemia.

### Lesions commonly seen in anterior cranial fossa

**Sinonasal malignancy**

**Epithelial:** Inverted papilloma, nasal polyposis, nasopharyngeal carcinoma

**Nonepithelial:** Olfactory neuroblastoma, juvenile nasopharyngeal angiofibroma

### Lesions commonly seen in middle cranial fossa

**Sellar and parasellar:** Pituitary adenoma [Figure 14], craniopharyngioma, cavernous sinus meningioma

**Juvenile nasopharyngeal angiofibroma, Nasopharyngeal carcinoma**

**Clivus and petro-occipital fissure:** Chordoma, Chondrosarcoma

### Lesions commonly seen in posterior cranial fossa

**Jugular foramina:** Paraganglioma, schwannoma

**Cerebellopontine angle tumors:** Schwannoma, meningioma, endolymphatic sac tumors

**Chordoma**

**Foramen magnum:** Meningioma

Few of the common pathologies that affect the base skull are discussed in this article.

### Congenital lesions

At about 8 weeks of gestation, a diverticulum of dura extends through the fonticulus frontalis into the prenasal

space. If regression and involution of this projection is incomplete, an embryologic fusion anomaly, such as a dermoid, glioma, or encephalocele occurs. Defect in the closure of the anterior neuropore results in a defect in the anterior fontanelle, foramen caecum, cribriform plate, sphenoid, and ethmoid bones.<sup>[4]</sup>

Nasal dermoid and sinus cyst result from defective involution of the dural tract and present as noncompressible masses over the nasal dorsum with an associated midline pit. Masses and pits may appear laterally on the nasal dorsum or distally down to the nasal tip. A small percentage of nasal dermoids show intracranial connection to the subarachnoid space. Nasal gliomas are benign glial heterotopias that present as noncompressible mass without intracranial communication.<sup>[2]</sup>

Encephaloceles are soft, compressible, and may enlarge with crying or with compression of the jugular veins. These are usually located in the midline and most commonly occipital in location –occipital encephalocele. Sincipital (frontoethmoidal) encephaloceles have a facial component and typically require a combined approach with craniotomy for repair and reconstruction.<sup>[4]</sup>

MRI is the best imaging modality for defining the contents and the intracranial connection of an encephalocele. MR accurately differentiates meningocele from encephalocele [Figure 15]. The extent of cerebral tissue in an encephalocele is also better defined with MRI, which aids in prognosis and surgical planning. High-resolution CT may be used to display the bone anatomy.<sup>[1]</sup>

#### Trauma and CSF leaks

Skull base fractures are rare and accounts for only 4% of severe head injury cases. Temporal bone is frequently involved. These fractures may be associated with CSF leaks. CT is the imaging technique of choice to display orientation and displacement of fracture fragments. Fracture of the skull base can be the direct extension of skull fractures or by indirect transmission from the mid-face to the skull base.<sup>[2]</sup>

Cerebrospinal fluid (CSF) leak or fistula is the exit of CSF from the intracranial cavity through an osseous defect within the skull base. It is secondary to disruption of the underlying dura arachnoid mater, resulting in a communication between the intracranial cavity and either the nasal or the middle ear cavity. Leakage of CSF into either the nose or the ear has been termed CSF rhinorrhea or otorrhea, respectively.<sup>[2]</sup>

CSF leaks can be traumatic or nontraumatic or spontaneous. The most common sites of injury involve the anterior cranial fossa, with fractures through the frontal sinus or cribriform plates [Figure 16]. In central skull base, fracture involving the roof of sphenoid sinus can result in CSF leak. Fractures



**Figure 13 (A, B):** Axial (A) and coronal (B) multiplanar reconstruction CT reveal sclerotic metastasis (black arrow) secondary to carcinoma prostate

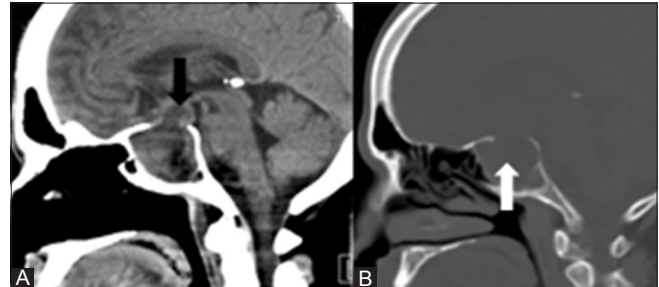


**Figure 14 (A, B):** Sagittal multiplanar reconstruction CT soft tissue (A) and bone window (B) reveal cystic pituitary adenoma (black arrow) extending in the sphenoid sinus (white arrow) through bony defect in roof of sphenoid sinus

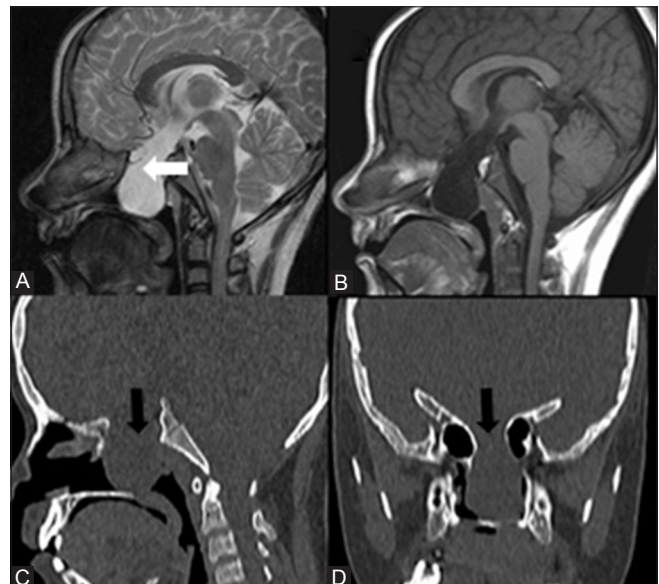


**Figure 15 (A-D):** Sagittal T2 (A) and T1WI (B) reveal transsphenoidal meningocele (white arrow). Sagittal (C) and coronal (D) CT bone window excellently demonstrate the bony defect (black arrow)

of temporal bone can result in CSF leak communicating with the middle ear complex and mastoid. Nontraumatic CSF leaks can be seen in normal or increased intracranial pressure and can be secondary to tumors, infection, or congenital lesions.

Multidetector CT is the first or may be the only study used to localize the site of the skull base defect and CSF leak.



CT cisternography is the modality of choice for evaluation of CSF fistula. Thin-section coronal and axial CT images in both prone and supine positions through the region of interest are acquired before and after intrathecal nonionic contrast administration. A positive result involves the presence of a skull base defect and contrast opacification within the sinus, nasal cavity, or middle ear.

#### Skull base inflammation

Skull base infections are commonly observed among uncontrolled diabetes mellitus, immunosuppression, and chronic otitis externa. Usually sinonasal and middle ear infections spread to the skull base and are frequently caused by bacteria such as *Pseudomonas aeruginosa* or invasive fungal infections such as zygomycete or aspergillus. Invasive fungal infections spread through vascular or neuronal route with vascular irregularity, stenosis, and occlusion. Cavernous sinus thrombosis and brain infarcts can be fatal.<sup>[5]</sup>

CT scan is the modality of technique to detect bony involvement. Erosion, reactive bone formation, and sclerosis can be picked up on CT. MR detects marrow invasion, intracranial extension, and can differentiate fungal from other infection [Figure 12]. Marked T2 shortening is diagnostic of fungal infection in appropriate clinical settings. Mucosal thickening and fluid levels can be identified within the sinus in pyogenic infection. Reactive sclerosis of sinus wall is seen in chronic infective process. Aggressive fungal infection often involves maxillary and ethmoidal sinuses followed by frontal and sphenoid sinuses.<sup>[2]</sup>

#### Polyposis

Polyposis is associated with super added noninvasive fungal infection [Figure 17], which may extrude in the anterior cranial fossa. The sinus wall shows expansion, remodeling, and at places may give away with intracranial extension.

#### Wegner's granulomatosis

Wegner's granulomatosis is a necrotizing granulomatous vasculitis affecting upper and lower respiratory tract associated with renal glomerulonephritis. The imaging features are nonspecific. Reactive bone sclerosis and thickening of the sinus wall [Figure 18] may be seen on the background of chronic sinusitis on CT scan.<sup>[2]</sup>

### Tumors Involving the Skull Base

#### Juvenile nasopharyngeal angiofibroma (JNAF)

These are locally aggressive benign vascular tumors seen in the adolescent boys. These tumors often arise in relation to the sphenopalatine foramen and extend in the pterygopalatine fossa and cause bowing of posterior wall of maxillary sinus [Figure 19]. Usually internal maxillary artery supplies the tumor. Anteriorly the growth extends into the nasopharynx and nasal cavity. Superiorly the tumor extends into the sphenoid sinus. The cavernous sinus may

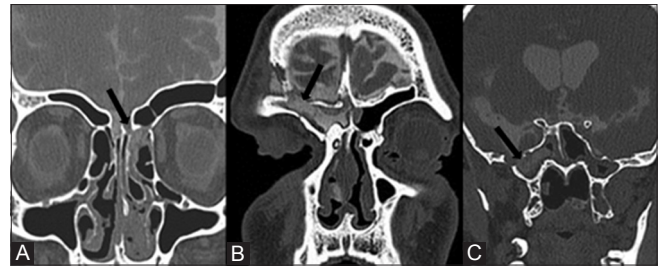


**Figure 16 (A-C):** Coronal multiplanar reconstruction CT reveal site of CSF leak (black arrows) through cribriform plate (A) posterior wall of frontal sinus (B) and superolateral wall of sphenoid sinus (C)

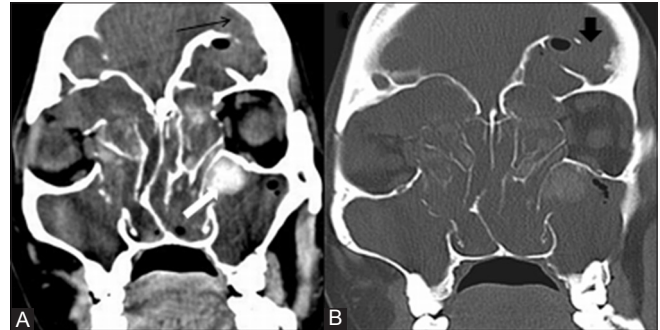


**Figure 17 (A, B):** Coronal CT soft tissue (A) and bone window (B) reveal fungal sinusitis with hyperdense concretions (thick white arrow) and break in wall of frontal sinus (thick white arrow) with extradural extension (thin black arrow) in anterior cranial fossa in a case of allergic fungal sinusitis



**Figure 18:** Coronal multiplanar reconstruction CT reveal nonspecific mucosal thickening in sphenoid sinus (white star), posterior nasal cavity with thickening, and sclerosis of sphenoid septae (black arrow)

become invaded. Along the lateral aspect, extension of the tumor in the infratemporal fossa can be seen through the pterygomaxillary fissure. Occasionally, the greater wing of sphenoid may be eroded exposing the dura with middle

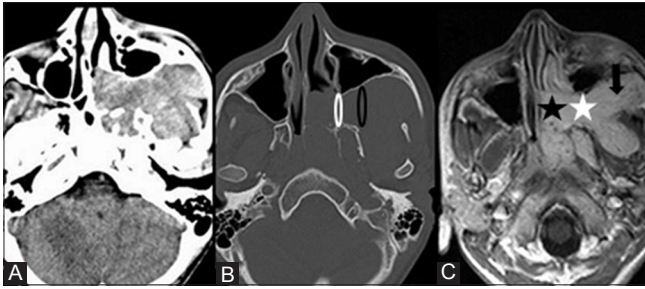


**Figure 19 (A-C):** Postcontrast axial CT soft tissue (A), bone window (B), and axial T1WI (C) reveal homogeneously enhancing mass in posterior nasal cavity (black star) with widening of sphenopalatine foramen (white circle) and pterygopalatine fossa (white star) in a case of juvenile nasopharyngeal angiofibroma. It extends in infratemporal fossa (black arrow) through pterygomaxillary fissure (black circle)

cranial fossa extension. Extension of the tumor in the inferior orbital fissure is seen with subsequent extension into the superior orbital fissure and middle cranial fossa.<sup>[5]</sup>

On postcontrast CT scan, JNAF reveals intense homogeneous enhancement. Bowing of the posterior wall of the maxillary sinus and pressure erosion of pterygoid plates are better appreciated on CT scan. Intracranial extension of the mass and cavernous sinus involvement is better appreciated on MRI.<sup>[2]</sup>

### Meningioma

Meningiomas are benign and the common neoplasms of the skull base that arise from arachnoidal cells of the meninges. Meningioma in the ASB is seen to erode the cribriform plate to extend into the ethmoidal sinus and nasal cavity. In the CSB, common sites of origin include the planum sphenoidale, tuberculum sellae, clinoid processes, and sellar diaphragm. Sellar meningiomas push and compress the pituitary gland against the sellar floor.<sup>[2]</sup>

Hyperostosis and adjacent dural thickening are common associated features in meningioma. In the posterior fossa, these tumors can be seen along the tentorium, cerebellopontine angle, petroclival, and foramen magnum.<sup>[2]</sup>

Reactive sclerosis and remodeling seen in meningioma is demonstrated by CT scan. Meningioma can extend along the cranial nerves with resultant widening and erosion of the neural foramina. These tumors can involve the cavernous sinus and encase the internal carotid arteries. Meningioma usually appears hypo- to isointense on T2-weighted images. Postcontrast scan shows intense homogeneous enhancement of the mass on both CT and MRI [Figure 20]. Often dural tail sign is seen on postcontrast scan.

### Sinonasal tumor extending into the anterior cranial fossa

Tumors of the nasal cavity or ethmoid sinus can easily erode the cribriform plate and fovea ethmoidalis to reach the anterior cranial fossa. The common tumors involving

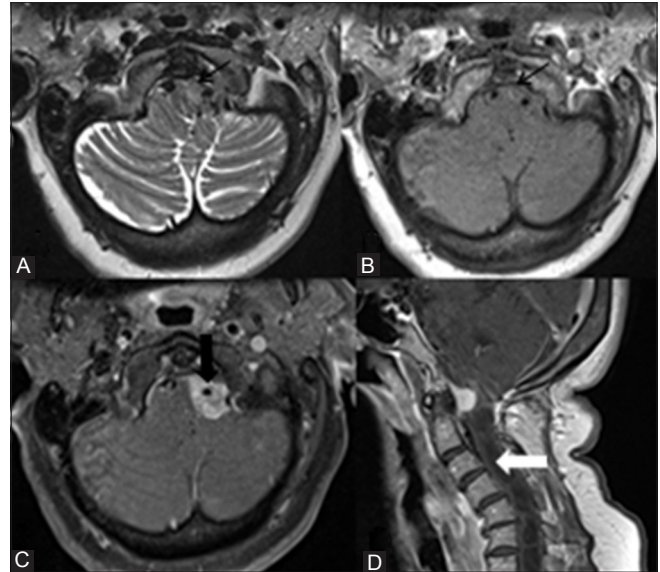


**Figure 20 (A-D):** An oval T2 hypointense (A) and T1 isointense (B) dural-based mass (thin black arrow) is seen in the anterior part of foramen magnum with homogeneous postcontrast enhancement (C and D) suggestive of meningioma. It causes encasement of left vertebral artery (thick black arrow) and compression of cervicomedullary junction with resultant cervical syrinx (white arrow)

the roof of the nasal cavity include inverted papilloma, squamous cell carcinoma, esthesioneuroblastoma, and lymphoma.<sup>[5]</sup>

Bone destruction with aggressive periosteal reaction seen in malignant tumor while remodeling and scalloping of the bones seen in benign tumor is depicted on CT scan. CT often underestimates the extent of skull base involvement. Marrow involvement is better delineated on MR imaging using T1-weighted images. Normally the bones of skull base appear hyperintense on T1-weighted images due to fatty marrow. Infiltration into bone results in replacement of fatty marrow with resultant T1 hypointensity. On MRI, malignant tumors are often heterogeneous or intermediate on T2W images. Hemorrhage may be depicted on gradient images. On postcontrast scan, variable enhancement is seen. Dural invasion and perineural spread are well delineated on postcontrast MRI. Peripheral tumor cysts when seen at tumor brain interface of the intracranial mass are highly suggestive of esthesioneuroblastoma [Figure 21].

### Nasopharyngeal carcinoma (NPC)

NPC is the most common malignancy involving the nasopharynx arising from pharyngeal epithelium. NPC usually presents late in the stage of the disease. Eighty-two percent of NPC arise in the posterolateral recess of the pharyngeal wall (Rosenmuller fossa), and 12% arise in the midline. NPC often infiltrates the PPF through the sphenopalatine foramen. Once the tumor is in the PPF, the maxillary nerve is at risk. Perineural spread can occur along cranial nerve V2 through the foramen rotundum into the

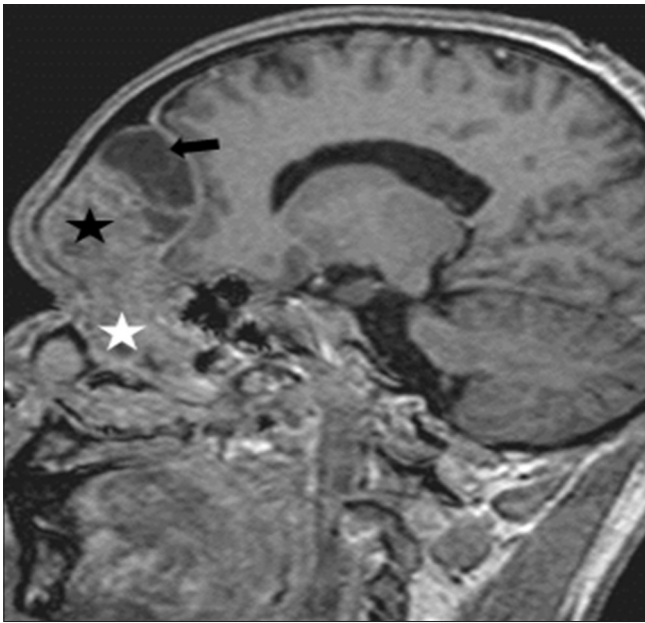


**Figure 21:** Postcontrast sagittal T1WI reveals a heterogeneously enhancing mass in superior nasal cavity (white star) with extension in anterior cranial fossa (extradural spread; black star) and presence of cysts (black arrow) at tumor brain interface in a proven case of esthesioneuroblastoma

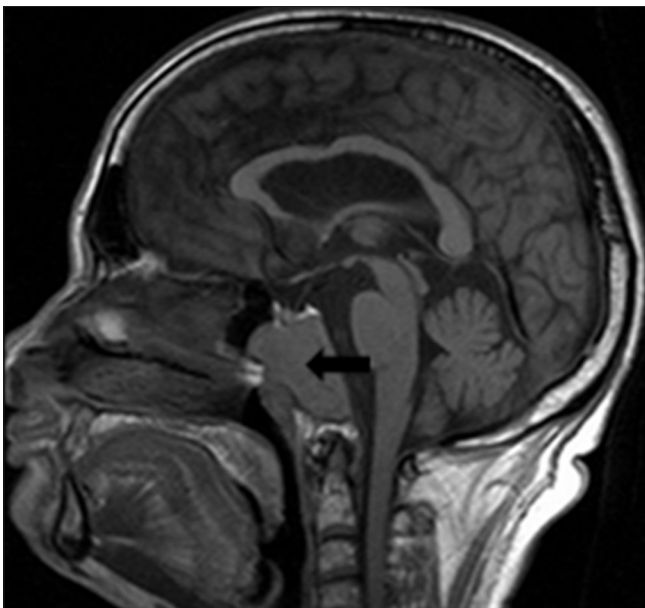


**Figure 23:** T1W sagittal image reveals T1 isointense expansile mass lesion replacing the clival marrow (black arrow) in a case of chordoma

intracranial cavity. Tumors can spread superiorly to the inferior orbital fissure, the orbital apex, and intracranially via the superior orbital fissure. NPC commonly spreads superiorly into the intracranial cavity or laterally into the masticator space. Once the tumor reaches the masticator space, perineural infiltration along cranial nerve V3 can be seen. The foramen lacerum is one of the most resistant tissues to tumor infiltration.<sup>[5]</sup>

MRI is the modality of choice for the diagnosis of NPC. Even

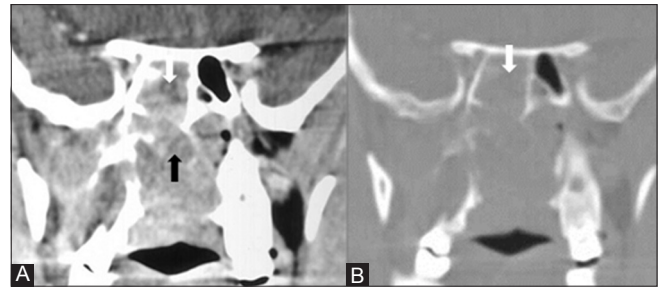


**Figure 22 (A, B):** Coronal multiplanar reconstruction CT postcontrast (A) and bone window (B) reveal heterogeneously enhancing nasopharyngeal mass (black arrow) extending in the sphenoid sinus (white arrow) in a case of nasopharyngeal carcinoma

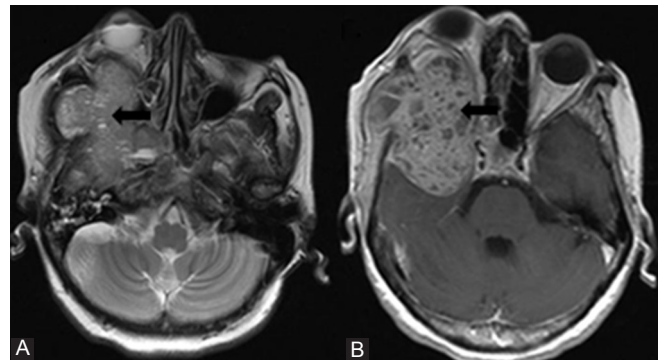


**Figure 24 (A, B):** Axial T2 (A) and postcontrast T1WI (B) reveal lobulated T2 intermediate to hyperintense mass involving the anterior and central skull base (black arrow) with homogeneous enhancement and mass effect on right orbit in a proven case of chondrosarcoma

subclinical cancers, which may be missed on endoscopy, can be detected by MRI. NPC display intermediate signal intensity on T2-weighted images and are low signal intensity on T1-weighted images. Postcontrast enhancement of the tumor is usually less than normal mucosa. MRI is superior to detect perineural tumor spread and intracranial detection.

CT is useful for detection of skull base tumor involvement [Figure 22]. However, it has now largely been replaced by MRI for primary and nodal staging. However, CT is still used for radiotherapy planning and monitoring patients after therapy and detecting NPC recurrence. With the introduction of 18F-FDG PET/CT in recent days, CT has reemerged in staging of the disease and to detect distant metastasis.

### Chordoma

Skull base chordomas are benign locally invasive neoplasms originating from embryonic remnants of notochord in the basisphenoid and may grow to involve multiple areas of the cranial base, and occasionally erode into the intradural space to encompass neurovascular structures and compress the brainstem. The relationship of the tumor to the internal carotid, vertebral, and basilar arteries, cavernous sinus, and brainstem determines the operability. The skull base chordomas can extend ventrally to the anterior cranial

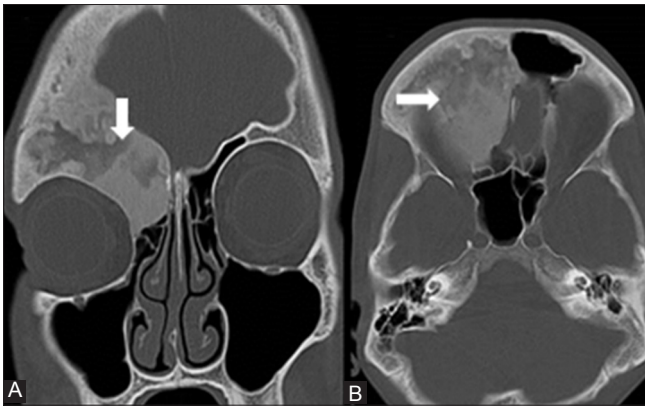


**Figure 25 (A, B):** Coronal (A) and axial (B) CT bone window reveals expansion of right frontal bone with intact cortex, loss of corticomедullary differentiation, and mixed ground-glass appearance and sclerosis (white arrow) in a case of fibrous dysplasia

fossa or caudally involving the upper cervical spine. It may involve the petrosphenoclivus junction, petrous apex, occipital condyle, and jugular foramen. Most of the clival chordomas are completely extradural. However, some invade the dura mater or extend into the intradural space, causing mass effect on the brainstem.<sup>[2]</sup>

The classic appearance of clival chordoma with high-resolution CT is that of a centrally located, well-circumscribed, expansile soft-tissue mass arising from the clivus with associated extensive lytic bone destruction [Figure 23]. Intratumoral calcifications indicate bone destruction rather than dystrophic tumoral calcifications. However, the chondroid variant may demonstrate real intratumoral calcifications. There is moderate to marked enhancement following administration of iodinated contrast material.<sup>[1]</sup>

MRI is the single best modality for radiologic evaluation of skull base chordomas. The chordomas display T2 hyperintense signal, which is likely to represent the high fluid content of the tumor. Chondroid chordomas may not be as bright as typical chordomas on T2-weighted images. On T2-weighted imaging, differentiation of tumor from adjacent neural structures is possible. Postcontrast scan shows moderate-to-intense enhancement, which may resemble “honeycomb” appearance. Even though multiple synchronous tumors or drop metastases from an intracranial chordoma are very rare, screening of the whole spine at the initial evaluation of a skull base chordoma is suggested.

### Chondrosarcoma

Chondrosarcoma are commonly found in various synchondroses. These tumors have a propensity for the petro occipital synchondrosis or fissures. Thus,

in contrast with chordoma, chondrosarcomas are off midline. On CT scan, they appear as well-defined lytic lesion with chondroid calcification. Chondrosarcoma displays hyperintense signal on T2, hypointense signal on T1-weighted images, and intense heterogeneous postcontrast enhancement [Figure 24].<sup>[2]</sup>

### Fibrous dysplasia (FD)

FD is a well-defined intramedullary, expansile fibro osseous lesion. The skull and facial bones are the affected sites in 10-25% of patients with monostotic fibrous dysplasia and in 50% of patients with polyostotic fibrous dysplasia. Complications of FD include occasional pathologic fracture and rare malignant degeneration.<sup>[2]</sup>

On CT scan, FD may have predominant ground-glass pattern, the homogeneously dense pattern, and the cystic pattern [Figure 25]. MRI features of FD are variable and confusing and may mimic a malignant tumor. Typically MRI shows an intermediate or low signal on T1-weighted images depending on the proportion of fibrous tissue to mineralized matrix. FD displays intermediate to high signal on T2-weighted images. High signal on MRI correspond to nonmineralized areas and regions of cystic change. Postcontrast scan shows heterogeneous enhancement. The radiologist should be aware of imaging features of FD, especially MR features, so that unwanted biopsy and surgeries can be avoided.

### References

1. Harnsberger R, Hudgins P, Wiggins R, Davidson C. Diagnostic Imaging: Head and Neck, 1e. Salt Lake City, USA: AMIRSYS; 2004.
2. Som PM, Curtin HD. Head and Neck Imaging. USA: Elsevier Health Sciences; 2002.
3. Borges A. Imaging of the central skull base. *Neuroimaging Clin N Am* 2009;19:441-68.
4. Laine FJ, Nadel L, Braun IF. CT and MR imaging of the central skull base. Part 2. Pathologic spectrum. *Radiographics* 1990;10:797-821.
5. Chong VF, Khoo JB, Fan YF. Imaging of the nasopharynx and skull base. *Neuroimaging Clin N Am* 2004;14:695-719.
6. Parmar H, Gujar S, Shah G, Mukherji SK. Imaging of the anterior skull base. *Neuroimaging Clin N Am* 2009;19:427-39.
7. Bou-Assaly W, Srinivasan A, Mukherji SK. Head and neck high-field imaging: Oncology applications. *Neuroimaging Clin N Am* 2012;22:285-96.
8. Hanna E, Vural E, Prokopakis E, Carrau R, Snyderman C, Weissman J. The sensitivity and specificity of high-resolution imaging in evaluating perineural spread of adenoid cystic carcinoma to the skull base. *Arch Otolaryngol Head Neck Surg* 2007;133:541-5.

**Cite this article as:** Raut AA, Naphade PS, Chawla A. Imaging of skull base: Pictorial essay. *Indian J Radiol Imaging* 2012;22:305-16.

**Source of Support:** Nil, **Conflict of Interest:** None declared.